Polymer Testing 103 (2021) 107367

Contents lists available at ScienceDirect

Polymer Testing

journal homepage: www.elsevier.com/locate/polytest

Antimicrobial PVDF nanofiber composites with the ZnO - vermiculite - chlorhexidine based nanoparticles and their tensile properties

Karla Čech Barabaszová [a,*], Sylva Holešová [a], Marianna Hundáková [a], Kamila Hrabovská [b], Lukáš Plesník [a,e], Dušan Kimmer [c], Kamil Joszko [f], Bożena Gzik-Zroska [d], Marcin Basiaga [d]

[a] Nanotechnology Centre, CEET, VŠB - Technical University of Ostrava, 17. listopadu 15/2172, 708 00, Ostrava - Poruba, Czech Republic
[b] Department of Physics, VŠB - Technical University of Ostrava, 17. listopadu 15/2172, 708 00, Ostrava - Poruba, Czech Republic
[c] Centre of Polymer Systems, Tomas Bata University in Zlín, třída Tomáše Bati 5678, 760 01, Zlín, Czech Republic
[d] Department of Biomaterials and Medical Devices Engineering, Silesian University of Technology, Roosevelta 40, 41-800, Zabrze, Poland
[e] Faculty of Materials Science and Technology, CEET, VŠB - Technical University of Ostrava, 17. listopadu 15/2172, 708 00, Ostrava - Poruba, Czech Republic
[f] Department of Biomechatronics, Faculty of Biomedical Engineering, Silesian University of Technology, Roosevelta 40, 41-800 Zabrze, Poland

ARTICLE INFO

Keywords:
PVDF nanofiber Materials
Mechanical properties
Antimicrobial and hydrophobic properties
Structural and phase characterization

ABSTRACT

The poly(vinylidene fluoride) (PVDF) nanofiber materials have attracted attention due to their enhanced and exceptional nanostructural characteristics. Electrospinning PVDF based nanofiber is one of the important new materials for the rapidly growing technology development such as nanofiber based conductive tissue engineering, scaffold materials, filters and medical textiles applications. At these areas the risk of microbial contamination is very high, hence in this study the PVDF nanofiber materials with antimicrobial zinc oxide (ZnO), zinc oxide/vermiculite (ZnO/V), zinc oxide/vermiculite-chlorhexidine (ZnO/V_CH) and vermiculite-chlorhexidine (V_CH) nanofillers were prepared by electrospinning, via one-step electrospinning process. The PVDF nanofiber diameters and their orientation were investigated using scanning electron microscope (SEM). The ZnO/V_CH and V/CH nanofillers with positive ζ - potential values were incorporated into PVDF nanofibers with an average diameter of 108 nm for PVDF_ZnO/V_CH and 100 nm for PVDF_V_CH samples. In contrast, ZnO and ZnO/V nanofillers with negative ζ - potential values reacted intensively with PVDF polymer. The slightly hydrophobe character was demonstrated by water contact angle from ~100°. The chemical interactions were evaluated by the Fourier transform infrared spectroscopy (FTIR). The presence of the β-phase in the original PVDF and the small traces of the α-phase in PVDF_ZnO and PVDF_ZnO/V samples was confirmed. In the PVDF_ZnO/V_CH and PVDF_V/CH samples where the specific interaction of PVDF chains with CH a rapid decrease in the β-phase fraction was evaluated. The mechanical properties based on the Young's modulus (E) and tensile strength (Rm) values were evaluated from the tensile test curves. Antimicrobial activity (longer than 48 h) against *S. aureus* and *E. coli* for PVDF_ZnO/V_CH and PVDF_V/CH samples was obtained.

1. Introduction

The process of electrospinning is one of the most frequently used, technologically and time-saving processes for the production of nanofibrous materials. Its significant progress is mainly due to the financial unpretentiousness, industrial production capability and technological variability enabling the regulation of the electrospinning parameters which consequently affect the properties of nanofibrous materials.

During the electrospinning, a high voltage source is used to inject a charge of a certain polarity into a polymer solution, which enables the solution to accelerate towards a collector of opposite polarity. The electrical force surpasses the surface tension of the polymeric solution, the Taylor's cone is formed, and a fibre jet is ejected from the head of the syringe. The solvents evaporated from the polymer solution leading to the solid polymer fibres coated on the collector, e.g. nonwoven substrate [1]. During the electrospinning process, the parameters such as the relative humidity, polymer concentration, electric potential, temperature, injection rate and distance between the tips (nozzles), which affect finally the mechanical, physicochemical properties and crystalline phases of the polymer fibers are controlled [2]. These main parameters also affect the fibers diameters (ranging from a few nanometers to several micrometers) [3] and various morphologies including beaded

* Corresponding author.
E-mail address: karla.cech.barabaszova@vsb.cz (K. Čech Barabaszová).

https://doi.org/10.1016/j.polymertesting.2021.107367
Received 25 May 2021; Received in revised form 14 September 2021; Accepted 26 September 2021
Available online 1 October 2021

fibers, porous fibers, ribbon fibers, side-by-side fibers, hollow fibers, hierarchical fibers, core-sheath fibers and/or crimped fibers [3].

Poly(vinylidene fluoride) (PVDF) is a semicrystaline polymer with a repeated units of $-(CH_2CF_2)_n-$, that usually contains 59.4 wt% of fluorine and 3 wt% of hydrogen [4]. PVDF as micro/nano-fiber material is intensively used for its high solubility in many common organic solvents (such as *N,N*-dimethyl acetamide (DMAc), *N,N*-dimethyl formamide (DMF) and *N*-methyl-2-pyrrolidone (NMP)) enables the electrospinning of PVDF to be performed easy [5]. The PVDF polymer has 4 phases - α, β, γ and δ. This polymer usually exists in α-phase, but using an electrospinning method (in presence of a suitable electric field) the PVDF polymer can be converted from α to β-phase [6]. Their high mechanical strength, good chemical resistance and thermal resistance allows used them in various industrial application as polymeric membrane electrolyte fuel cell [1], chemical sensors [3], desalination [7], separation membranes [5] and mainly as materials for filtration [3,8]. It should be mentioned that many PVDF membranes for industrial processes are made from inorganic (nano)materials and/or organic polymers [5].

Inorganic nanoparticles, including SiO_2, ZnO, Al_2O_3, TiO_2, Fe_2O_3, etc., reinforce mechanical properties (mechanical strength) of PVDF materials due to chemical and physical interactions between nanoparticles and polymer. For example, just 1.5 wt% of the hydrophilic and hydrophobic SiO_2 nanoparticles in PVDF nanofibers led to an increase in average nanofiber diameters, good dispersion and the higher compatibility of the hydrophilic silica nanoparticles. According to the result of the tensile test, the break strength increased from 1.61 MPa to 2.39 MPa, while the elongation at break decreased from 257% to 160% [9]. The SiO_2 nanoparticles also changed PVDF crystal formation during the electrospinning process when they contributed to the phase transformation from α-phase to β-phase. Similar results were obtained in the case of Al_2O_3 nanoparticles, which also caused the better mechanical and thermal properties as well as the hydrophilicity, permeability and fouling resistance [10]. The ZnO nanoparticles during electrospinnig significantly affected the electrostatic conditions resulting in an increase in the number of beads in PVDF nanofibers. Nevertheless, the nanofibers had high quality, uniform morphology and nanometer diameters. Until now, PVDF nanofibers with ZnO nanoparticles have been used for piezoelectric nanogenerators with high output power [11].

The clay particles as inorganic nanostructured materials are widely used and have a very important role in the field of polymer nanocomposites. In the case of the PVDF nanofiber materials, halloysite [12], cloisite (montmorillonite clay) [13], vermiculite [14] and zeolite particles [15] have been applied. This is because clay particles display high adsorption capacity, high surface area and unique chemical composition with microporosity, layered structures, and small (nanoscale) sizes. The dispersion of clay particles into the polymer matrix has a key effect on nanofiber materials due to the clays are generally hydrophobic and it is difficult to disperse them homogenously. For these reasons, the surface of clay particles is modified with organic modifiers (functionalized) or equipment as homogenizer or sonicator are used for achieving homogenous dispersions [16]. Targeted selection of the functionalized nanofillers based on the inorganic, organic or their hybrid form applied to the PVDF nanofiber materials extends their applications also to medical areas (such as materials for medical treatment or drug delivery) or the packaging and textile industry.

The main aims of the present work were to develop new antimicrobial PVDF nanofiber materials (active against *Staphylococcus aureus* and *Escherichia coli* as the most common strains reacting on contact with the human body) with incorporated nanofillers based on ZnO-vermiculite-chlorhexidine prepared by the electrospinning, via one-step electrospinning. The main idea of the work was to monitor the influence of identical electrospinning conditions on the structural and phase changes of PVDF nanofiber materials with different types of antimicrobial nanofillers. Attention was focused on finding connections between particle size and ζ - potential value of nanofillers with respect to the changes of PVDF crystal phase, nanofiber diameter, morphology, and mechanical properties.

2. Materials and methods

2.1. Nanofillers particles preparation

Four nanofiller particles types were used for PVDF nanofiber materials preparation: zinc oxide, zinc oxide/vermiculite, zinc oxide/vermiculite-chlorhexidine and vermiculite-chlorhexidine.

First nanofiller, zinc oxide nanoparticles (ZnO, Bochemie s.r.o., Czech Republic), were obtained as a commercial sample from recycled processes of the chemical compounds.

Next three nanofillers (respectively, nanocomposite samples) were prepared by the following steps. The natural Mg-vermiculite from Brazil (V, Grena Co., Veselí nad Lužnicí, Czech Republic) with sievied fraction <40 μm was used as the starting material. 5 g of vermiculite with 15 g of dihydrate zinc acetate ($(CH_3COO)_2Zn.\ 2H_2O$) and 15 g of anhydrous Na_2CO_3 (both from Sigma Aldrich) dispersed in 300 ml of distilled water were sonicated using the titanium sonotrode (UP100H from Hielscher, Teltow, Germany) for 15 min throughout the cycle at 50% amplitude. The dispersion was twice washed with distilled water and then dried at 75 °C for 24 h. The solid sample was calcined at 350 °C for 1.5 h and named the zinc oxide/vermiculite (ZnO/V) nanocomposite.

The ZnO/V nanocomposite sample was sonochemicaly intercalated by the following process: 2 g of chlorhexidine dihydrochloride (CH) dissolved in 50 ml of demineralized water were stirred with 50 ml of ethanol for 5 min. 7 g of the ZnO/V nanocomposite sample were added to the CH solution and ultrasound treatment using the titanium sonotrode for 15 min was applied. The final dispersion was freed from water/ethanol solution by centrifugation and drying at 75 °C for 24 h. The sample was named ZnO/V_CH nanocomposite. The V_CH nanocomposite sample was prepared exactly under the same conditions, where 7 g of natural Mg-vermiculite were used as starting material.

2.2. Preparation of the PVDF nanofiber materials

For the spinning process in electrostatic field, the solution of polyvinylidene fluoride (PVDF, Kynar, Arkema) in *N,N*-dimethylformamide (DMF, Lach-Ner, s.r.o., Czech Republic) with concentration 20 wt% was prepared. The electrical conductivity was adjusted on 104 μS/cm by means of sodium tetraborate decahydrate (Borax PENTA s.r.o., Czech Republic) and citric acid (PENTA s.r.o., Czech Republic). The solution was mixed with various nanofillers so that the content of nanofiller in the dry extract of the nanofiber material was 15 wt%. Ultrasound bath (60 min) and 3 h of intensive mixing were used for better dispersion of nanofillers in polymeric solution.

Nanofibers were prepared in a width of 20 cm from polymeric solution or dispersion by means of an electrospinning machine SpinLine 40 (CPS UTB Zlín, Czech Republic) using a nanofiber forming electrode equipped with 8 fiber forming nozzles. The used experimental conditions were: temperature 23 – 25 °C, relative humidity 32 – 35%, applied electric voltage 75 kV, dosing of polymer solution 0.19 ml min^{-1}, variable distance between electrode from 190 to 200 mm and speed of substrate collecting nanofibers 0.1 m min^{-1}. Nanofibers were collected on polypropylene (PP) nonwoven textiles with basis weight 30 g m^{-2}.

2.3. Characterization methods

The chemical composition of the nanofiller samples was obtained from elemental analysis by X-ray fluorescence spectroscopy (SPECTRO XEPOS new energy dispersive X-ray fluorescence spectrometer, WI, USA).

The particle size of the nanofiller samples was determined by the HORIBA Laser diffraction particle size analyzer (LA-950 instrument, Kyoto, Japan) with a two short-wavelength blue and red-light sources in conjunction with forward and backscatter detection. The particle size

analyses were conducted with the refractive indices 1.54 (for vermiculite), 2.02 (for zinc oxide) and 1.33 (for water).

Zeta potential (ζ - potential) of the nanofiller samples was measured by a nanoparticle analyser (HORIBA Nanopartica SZ-100, Kyoto, Japan) equipped with a microprocessor unit to directly calculate the ζ - potential. 0.1 g of each nanofiller sample was mechanically mixed with 25 ml of distilled water. 0.1 ml of the suspension was introduced into the disposable zeta potential cell. Each data point is an average of 6 measurements realised at 24.3 °C.

Specific surface area (SSA) of the nanofiller samples was measured at nitrogen atmosphere by means of Thermo scientific Surfer (Dresden, Germany). The samples were degassed under vacuum (10^{-6} torr) at 80 °C for 24 h for the vermiculite sample and for other samples at 120 °C for 24 h. The SSA was calculated using the BET (Brunauer-Emmett-Teller) equation by assuming the area of the nitrogen molecule to be 0.1620 m^2.

The morphology of the nanofiller samples was investigated using a scanning electron microscope (SEM) QUANTA 450 SEG (FEI, France). The samples were coated with a gold/palladium film to avoid problems with electrical charging. SEM images were obtained using a scattered electron detector (SE).

The water contact angle (WCA, the test liquid) of PVDF nanofiber materials was measured using a three-point technique at 22 °C, 995 mba and relative humidity 60%. 0.1 ml of destiled water was deposited onto surface of the PVDF nanofiber materials using a micropipette, each drop (0.1 ml) was recorded using a videocamera Mitutoyo (Tokyo, Japonsko) and its images were evaluated using Pixel Fox program (Germany). The examined WCA are presented as a mean of 4 measurements per PVDF sample type. Two methods were used to analyse the contact angle. The first direct method was based on measuring the angle of the droplet tangent adjacented to the PVDF surface. The second indirect method was based on analyzing the dimensions of the droplet profile, which was replaced by a circle using software, and the contact angle was calculated based on the radius of the water drops adjacented to the PVDF surface and the height drop. Since identical results were obtained from both methods, the results of the first direct method are given here.

The X-ray powder diffraction (XRD) analysis of the nanofiller samples was performed using the diffractometer RIGAKU Ultima IV, Tokyo, Japan (CuKα radiation, Ni-Kβ filter, Bragg-Brentano arrangement, scintilation detector). Samples in the standard holder were measured in ambient atmosphere, operating conditions 40 kV and 40 mA. Samples were measured in the range 2θ 1.5 – 70°, scanning rate 2.7°/min, step width 0.02°. Phase analysis was evaluated by database PDF-2 Release 2011. Figures of the XRD patterns were drawn using Origin8Pro software.

The morphology of PVDF nanofiber materials was investigated using a scanning electron microscope Vega 3, Tescan, Czech Republic and in detail using scanning transmission electron microscope (STEM) JEOL JSM-7610F Plus, Tokyo, Japan. The samples were coated with a platinum film and the SEM images were obtained in low vacuum using a secondary electron detector (SE, LEI).

The FTIR spectra of PVDF nanofiber materials were measured by ATR (Attenuated Total Reflectance) technique. The nanofiber samples were laid and pressed by a pressure device on the single-reflection diamond ATR crystal. The IR spectra were collected using FT-IR spectrometer Nicolet iS50 (ThermoScientific, MI, USA) with DTGS detector with Smart Orbit ATR accessory. The measurement parameters were as follows: spectral region 4000 - 400 cm^{-1}, spectral resolution 4 cm^{-1}; 64 scans; Happ-Genzel apodization.

2.4. Antimicrobial activity of the PVDF nanofiber materials

The antimicrobial activity (AC) of all PVDF nanofiber materials was tested against the Gram-positive strain *Staphylococcus aureus (S. aureus*, CCM 4516) and the Gram-negative strain *Escherichia coli (E. coli,* CCM 4225), provided by the Czech collection of microorganisms (CCM).

The PVDF nanofiber materials were processed by a modified AATCC 100 test method for surface-treated materials (textiles with non-leachable additives, paper, granules, etc.). Prior to testing, suspensions of tested strains were prepared in Erlenmeyer flasks and were incubated for 24 h in a thermostat at 35 ± 2 °C. After incubation, using a densilameter, working suspensions at a concentration of 103 CFU/ml were prepared by dilution with saline. Subsequently, plastic containers with lids were prepared containing 30 ml of TSB broth with a microbe suspension with a concentration of 103 CFU/ml. Squares of tested nanofibers were placed in labeled vials and placed on a shaker. A first aliquot (2 x 1 ml) was taken 1 min after the nanofibers were suspended, the mixture was inoculated into a sterile petri dish and poured into 15 ml of TSA agar cooled to 45 ± 2 °C. Furthermore, samples were taken at the recommended intervals of 60, 120, 180, and 240 min after the start of the test. Additional samples were taken after 24 and 48 h. For better colony counting, a 10^{-1} dilution was made, and an aliquot was also taken from this dilution and embedded in TSA agar. All agars were cultured for 24 h in thermostat at 35 ± 2 °C. After incubation, the number of grown colonies was evaluated for all agars.

2.5. Mechanical properties of the PVDF nanofibers materials

The analysis of the mechanical properties of the PVDF nanofiller materials were carried out using the MTS Criterion Model 43 static testing machine. The tensile test was carried out in accordance with the recommendations of the PN-EN ISO 527 standard.

Each of the tested samples was fixed in the grip in such a way that the measuring distance between the holders was the same for each sample. The device handle ensures accurate and reliable fixing of the axis of the test device without the possibility of displacement during the test. The samples were subjected to a static tensile test at a speed of 50 mm/min. The results of force measurements were measured with an accuracy of 1 N. The measurement of each sample was repeated 10 times.

3. Results and discussion

3.1. ZnO-vermiculite-chlorhexidine nanofillers characterization

The four nanofiller types ZnO, ZnO/V, ZnO/V_CH and V_CH for the preparation of the PVDF nanofiber materials were selected. These nanostructured particles were selected with respect to the morphology, surface, and phase differences. The greatest emphasis was on surface properties such as ζ - potential (positive and/or negative values), relatively identical specific surface area (SSA) and particle size (evaluated based on mean d_{43} and mode d_m diameters values).

The zinc oxide (ZnO) nanoparticals formed spherical agglomerates with the specific surface area SSA = 52.7 $m^2.g^{-1}$, ζ - potential value −39.8 mV and the average diameter d_m = 10.1 μm. The individual ZnO nanoparticles (Fig. 1) had a platelet shape with crystallite size (Lc) 15.95 nm.

The irregularly shaped particles of the Mg - vermiculite (V) with the mode diameter d_m = 12.4 μm and specific surface area SSA = 90.6 $m^2.g^{-1}$ were used as the starting material for nanofiller samples preparation. The V particles with a structural formula $(Si_{6.32}Al_{1.58}Ti_{0.1})(Mg_{4.75}Ca_{0.34}Fe_{0.91})\ O_{20}\ (OH)_4\ (Ca_{0.04}\ K_{0.38})$ had a smooth surface, rounded edges and ζ - potential value 60.0 mV. The presence of smaller particles around bigger V particles is evident from the SEM image (Fig. 1), which confirmed the higher average diameter (d_{43}) of V particles on 13.5 μm.

The ZnO/V nanofiller samples with 21.9 wt% of the ZnO nanoparticles, which were homogenously grown on the vermiculite particle's edges and surfaces, were prepared by the sonochemical and heat treated process. The ZnO/V nanofiller particles with a bimodal particle size distribution with the mode diameters 0.172 μm and 10.10 μm formed agglomerates with mean diameter d_{43} = 9.1 μm, which corresponded to the ζ - potential value 20.6 mV. The specific surface area (SSA) of the

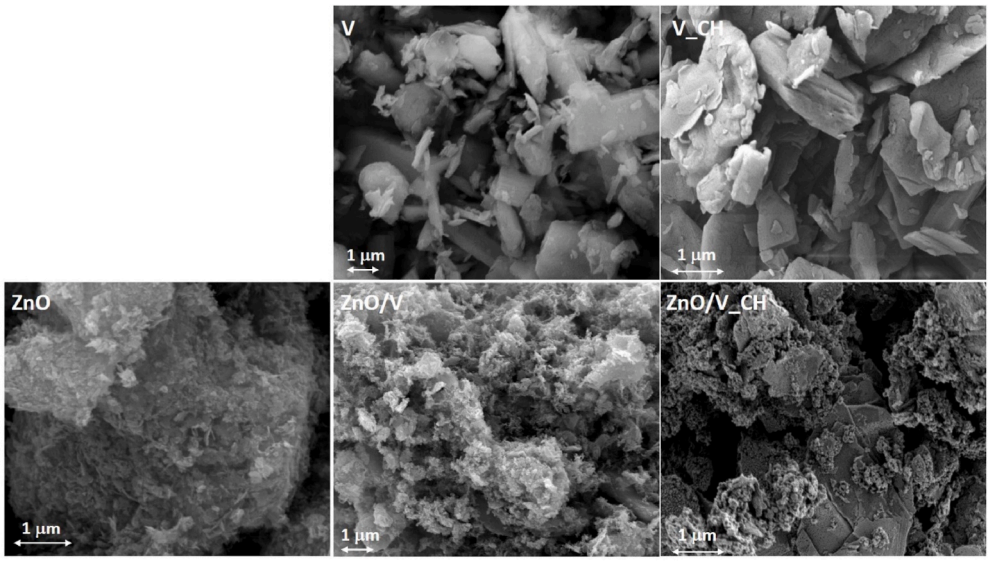

Fig. 1. SEM images of the natural Mg - vermiculite (V) particles, ZnO, ZnO/V, ZnO/V_CH and V_CH nanofiller samples.

ZnO/V nanofiller sample was 23.6 $m^2.g^{-1}$. The crystallite size (Lc) of ZnO nanoparticles in the ZnO/V nanofiller was 12.36 nm. The ZnO/V_CH nanofiller particles with 17.2 wt% of ZnO and 27.5 wt% of organic carbon content were formed by the very smooth surface and the sharp edges at the ends of V particles (Fig. 1). The ZnO/V_CH nanofiller particles created agglomerates with mean diameter 10.9 μm and bimodal particle size distribution with mode diameters 0.259 μm and 11.6 μm. The intercalation of CH leads to the positive ζ - potential value + 23.5 mV and to relative preservation of the specific surface area SSA = 24.3 $m^2.g^{-1}$. The crystallite size (Lc) of ZnO nanoparticles in the ZnO/V_CH nanofiller was 7.05 nm. Both ZnO/V and ZnO/V_CH nanofillers were characterized by sharp edges of the original vermiculite particles, which were caused by the directional growth of ZnO nanoparticles in these places. The nanofiller particles characteristic correspond to the authors results in Ref. [17].

The V_CH nanofiller particles with 28.1 wt% of organic carbon content exhibited narrow monomodal particle size distributions with the mean diameter d_{43} = 17.6 μm, mode diameter d_m = 16.2 μm, SSA 32.0 $m^2.g^{-1}$ and ζ - potential value +19.8 mV. The V_CH particles had (in contrast to the natural V particles) a smooth surface and the particle edges were sharp. The CH formed a brightening/visibility of the layered structure due to the intercalation of CH into the interlayer area.

XRD patterns (Fig. 2) of the ZnO and ZnO/V nanofiller samples show reflections of the hexagonal wurzite ZnO structure (PDF card no. 01-079-2205) about *2θ* 31.80°, 34.44° and 36.21° (*d*-values 0.281 nm, 0.260 nm and 0.247 nm). The ZnO/V nanofiller reflections shown at 7.31° 2θ (*d* = 1.210 nm) belong to V structure with ZnO formed in the V interlayer [18,19] and at 8.86° 2*θ* (*d* = 0.997 nm) confirmed dehydrated V structure after calcination at 350 °C [17]. Reflections of tremolite admixture phase (PDF card no.00-013-0437) at 10.50° and 28.55° 2*θ* (*d* = 0.842 nm and 0.312 nm) are observed for all V samples. Moreover, XRD pattern shows reflections assigned to intermediate products phases of $Zn_5(OH)_8(CH_3COO)_2{\cdot}2H_2O$ and $Zn_3(OH)_4(CH_3COO)_2$ [20,21] which were found in sample as result of incomplete ZnO formation during synthesis. XRD pattern of ZnO/V/CH shows very low intensive reflections at *2θ* 4.04°, 5.03° and 5.40° (*d* = 2.187 nm and 1.748 nm) as result of CH intercalation [22].

XRD pattern of V/CH nanofiller shows reflections at 2.99°and 3.985° 2θ (*d* = 2.950 nm and 2.216 nm) confirmed CH intercalated into the V structure [17]. Low intensive reflection at 6.14° 2θ (1.438 nm) shows the original V structure preserved. The next V reflections (PDF card no. 01-074-1732) are observed at 19.30°, 27.60° and 31.15° 2θ (*d* = 0.460 nm, 0.323 nm and 0.287 nm). XRD patterns of V/CH and ZnO/V/CH confirmed non-intercalated CH on the V particles surface.

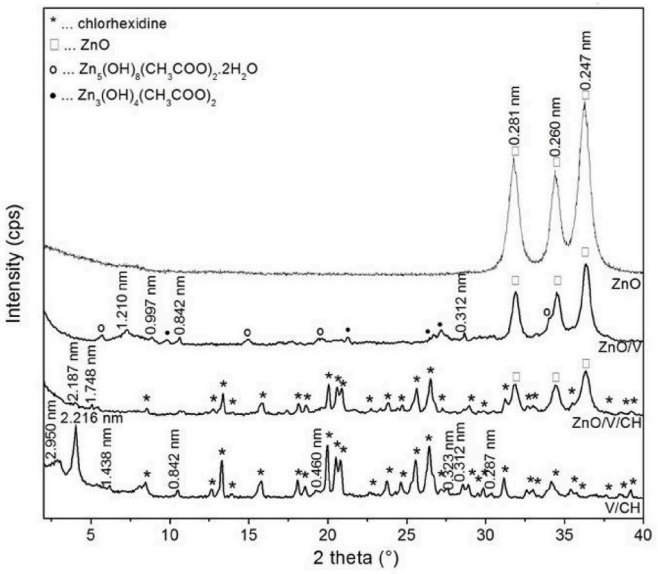

Fig. 2. XRD patterns of the ZnO, ZnO/V, ZnO/V_CH and V_CH nanofiller powder samples.

3.2. PVDF nanofiber materials characterization

The electrospinning PVDF nanofiber materials with different nanofillers obtained via one-step electrospinnig without involving any special collection method or post-spinning treatment were investigated using scanning electron microscope (SEM) and show Fig. 3 and in detail Fig. 4.

The nanofiber materials formed uniform/compact layers with different basis weights (gsm) ranging from 1.85 $g.m^{-2}$ for PVDF sample to 3.35 $g.m^{-2}$ for PVDF_V_CH sample (Table 1). In all samples, the presence of the voids with different sizes (respectively, the area without nanofibers) and droplets of the original PVDF was observed (the sizes were measured from the SEM images using JMicroVision image analyzer). In the samples PVDF, PVDF_ZnO and PVDF_V_CH, the voids reached the size of 12 - 30 μm, while in the sample PVDF_ZnO/V_CH

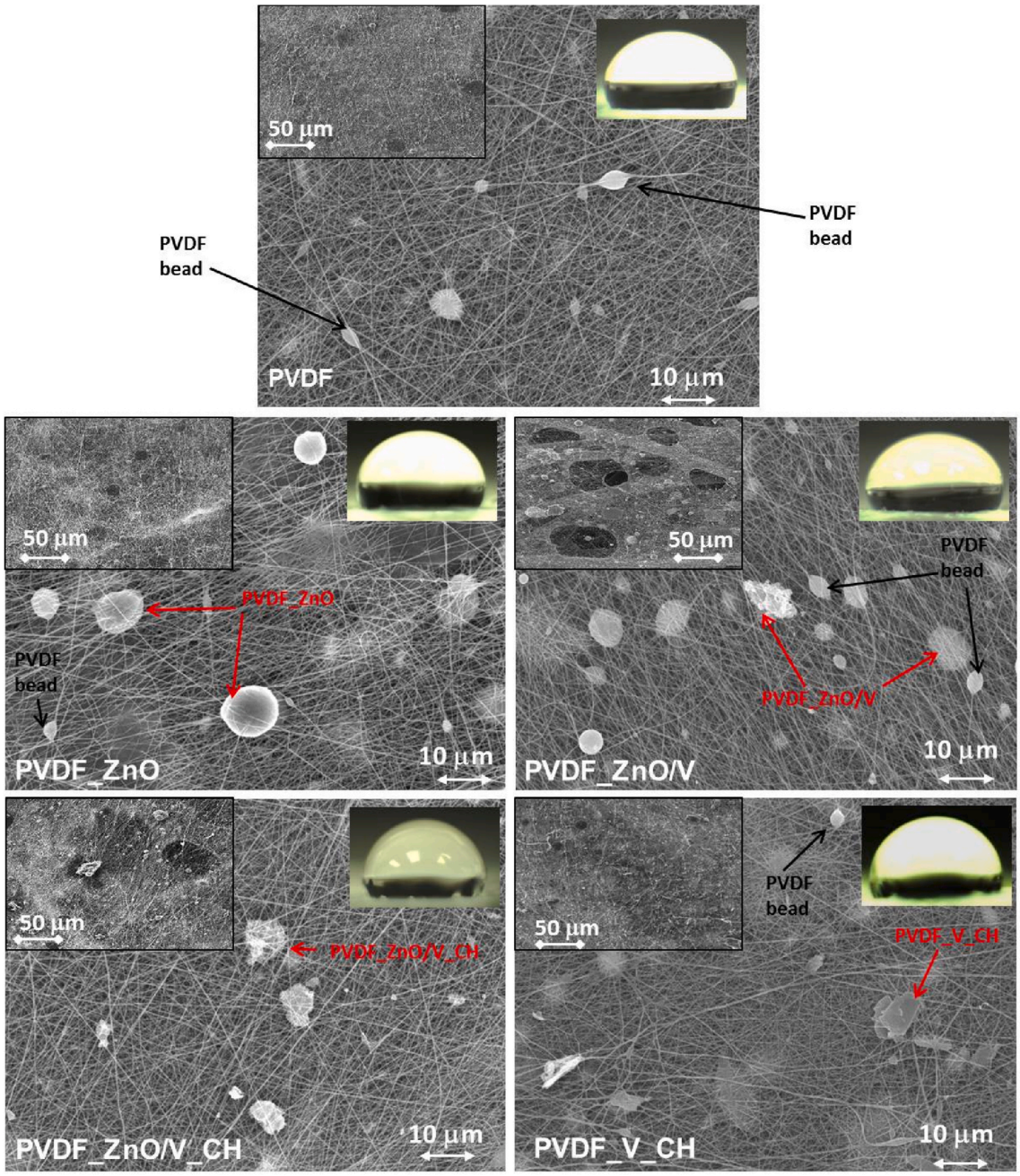

Fig. 3. SEM images of the original PVDF, PVDF_ZnO, PVDF_ZnO/V, PVDF_ZnO/V_CH and PVDF_V_CH nanofiber materials. Detail: SEM images of the PVDF voids and beads (left parts), the images of the water drops on the PVDF nanofiber material surfaces (right parts).

reached the size of 14 - 41 µm. Extended voids of the 73 - 48 µm and 25 - 20 µm were observed in the PVDF_ZnO/V sample. The PVDF beads (8 - 3 µm in size) (black line in Fig. 3) were observed in all nanofiber samples except the PVDF_ZnO/V_CH sample. The beads had a predominantly stretched droplet and/or ellipse shape, which passed into smooth fibers as a result of the optimal viscosity of PVDF solution. In addition, in the samples PVDF_ZnO and PVDF_ZnO/V sporadically occurred beads with a round-like shape with average size around 10 µm as results of low-viscosity of PVDF solution. The beads (droplets) formation in nano-fibrous structures is a known morphological phenomenon caused by the naturally change in viscosity of the PVDF solution during electro-spinning [7]. In the case of PVDF_ZnO/V, PVDF_ZnO/V_CH and PVDF_V_CH nanofiber materials, the positive effect of the vermiculite particles presence (as carriers of inorganic and organic nanostructured components) is evident. They contributed to the homogeneous distribution of individual nanofillers and their horizontal arrangement in the volume of PVDF nanofiber materials.

The water contact angles (WCA, wettability angle) on the PVDF nanofiber materials surfaces were used to determine wetting and water absorbency during time evolution. It is known that a surface with a contact angle smaller than 90° would be considered hydrophilic and larger than 90° would be considered hydrophobic. The images of water drops are seen in details of Fig. 3.

The PVDF nanofiber materials showed a very poor absorbency (wettability) of the water drops. It was manifested by preservating of the water drop shape on the PVDF and PVDF_ZnO surfaces, which remained unchanged for 1 h. The highest values of the WCA were measured for PVDF 110° ± 2.8 and 109° ± 2.5 for PVDF_ZnO nanofiber materials. For PVDF nanofiber materials containing V and ZnO also (PVDF_ZnO/V_CH, PVDF_ZnO/V), the time to absorb water drop was longer (15 s and 60 s,

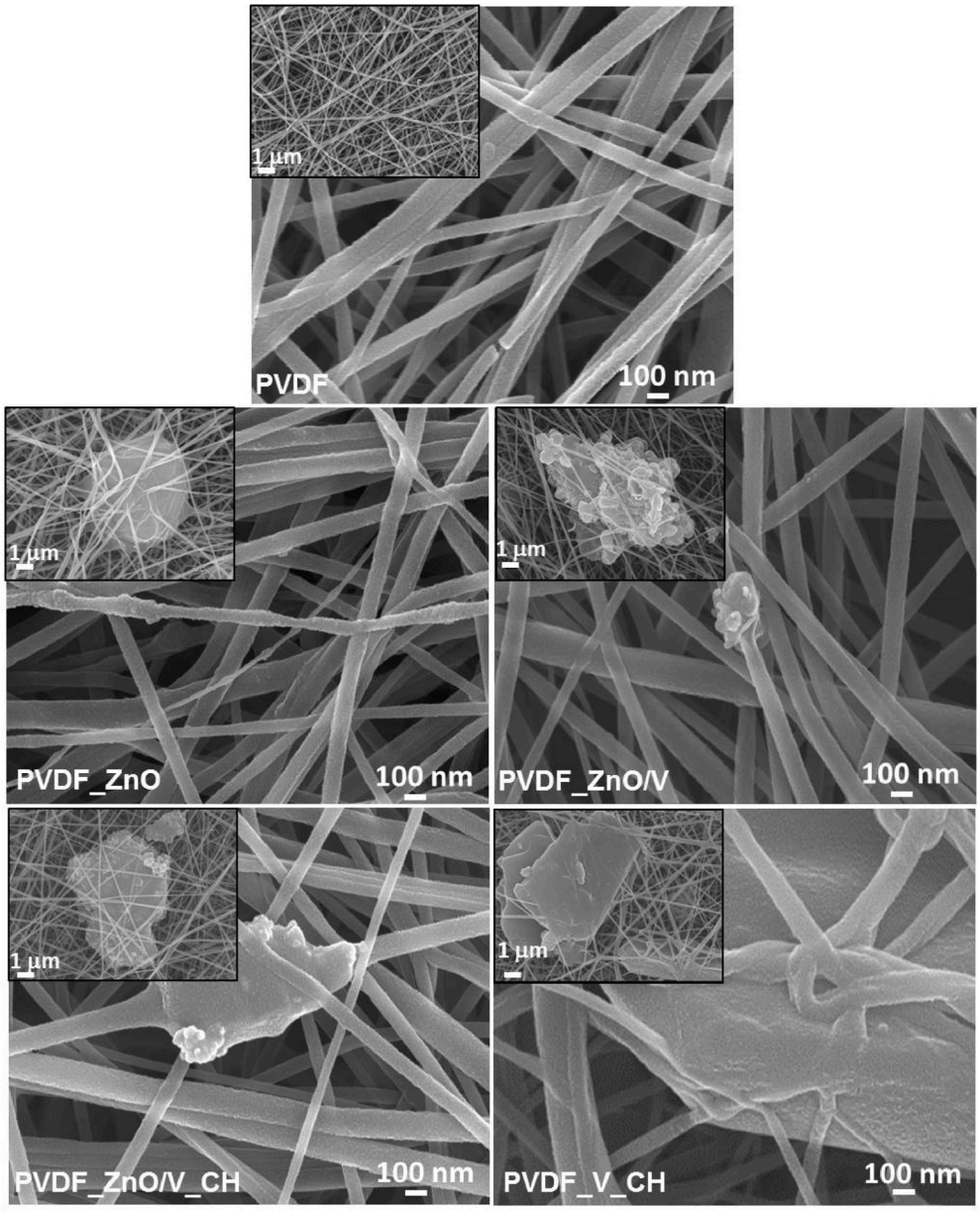

Fig. 4. The SEM images of the PVDF, PVDF_ZnO, PVDF_ZnO/V, PVDF_ZnO/V_CH and PVDF_V_CH nanofiber materials in details and different magnifications.

Table 1
The measured and evaluated parameters of the PVDF nanofiber materials.

Samples	gsm	Dmean ± S.D.	Dmode	Dmin	Dmax
	($g.m^{-2}$)	(nm)	(nm)	(nm)	(nm)
PVDF	1.85	89.2 ± 20.0	77.3	51.7	149.9
PVDF_ZnO	2.36	93.0 ± 26.3	116.3	30.9	153.9
PVDF_ZnO/V	3.00	107.1 ± 41.0	107.2	32.9	255.3
PVDF_ZnO/V_CH	2.00	108.7 ± 28.5	88.6	65.8	223.4
PVDF_V_CH	3.35	100.5 ± 34.9	109.7	28.3	261.3

respectively). The PVDF_V_CH nanofiber material took only 10 s to absorb the water drop. This wettability phenomenon is mainly explained by the presence of V particles as a layered material with a strong absorbent behavior. The water molecules intensively react with the vermiculite interlayer space and surface [22–24]. Due to the presence of ZnO nanoparticles on the vermiculite edges and at the same time chlorhexidine in the interlayer space, the absorption rate of the water drop changes and at the same time the water contact angle of the PVDF nanofiber materials decreases. The lower contact angles of 101° ± 1.0 for PVDF_ZnO/V, 100° ± 1.2 for PVDF_ZnO/V_CH and 101° ± 0.5 for PVDF_V_CH were measured. These measurements and observations confirmed the slightly hydrophobe behavior of all PVDF nanofiber materials prepared by the electrospining process.

Fig. 4 shows the cross-section SEM images characterising the arrangement and orientation of visible PVDF nanofiber materials and their interactions with different nanofillers. The diameters and structural changes of nanofibers are shown on the SEM images in higher magnification. The nanofibers diameters were measured from the SEM images using JMicroVision image analyzer (which are not listed in the SEM images) and evaluated using OriginPro statistical software. The 250 nanofibers of each PVDF sample were processed for the calculation. The average nanofiber diameters (Dmean) with standard deviations (S.D.), the most common diameters (Dmode), intervals of the minimum (Dmin) and maximum nanofiber diameters (Dmax) are shown in Table 1.

The original PVDF nanofiber materials have uniform nanofibers from evaluated PVDF nanofiber materials, most often with a diameter of 77

nm (Dmode). Very often, two fibers are joined (entwined) into one whole (bundle). The thinnest nanofibers (around 55 nm) have no uniform diameter over their entire length, they are deformed (curved) or completely torn.

The nanofillers contributed to the increased of the diameter of PVDF nanofibers, with the highest average values being measured in samples with nanofillers containing vermiculite particles (PVDF_ZnO/V, PVDF_ZnO/V_CH and PVDF_V_CH), Dmean ~ 100 – 108 nm. The nanofibers did not change the diameter throughout their visible length and were not deformed.

The greatest disunity in nanofiber diameters was observed for the PVDF_ZnO sample as a result of the agglomeration behavior of ZnO nanoparticles, which was not prevented even by homogenization with the ultrasonic bath during the preparation of the PVDF solution. From the SEM image (Fig. 4), it is seen that non-agglomerated ZnO nanoparticles are anchored on the walls of the PVDF nanofibers, where they cause their wrinkling, changes in their thickness respectively. In these the thickness values correspond to the structural changes in the PVDF nanofiber samples places, 3.8 wt% Zn, 8.6 wt% O, 66.9 wt% C and 20.7 wt% F were measured using EDS elemental analysis. At the same time, in other parts, the non-agglomerated ZnO nanoparticles lead to a reduction of nanofibers diameters. In these places, nanofibers were markedly

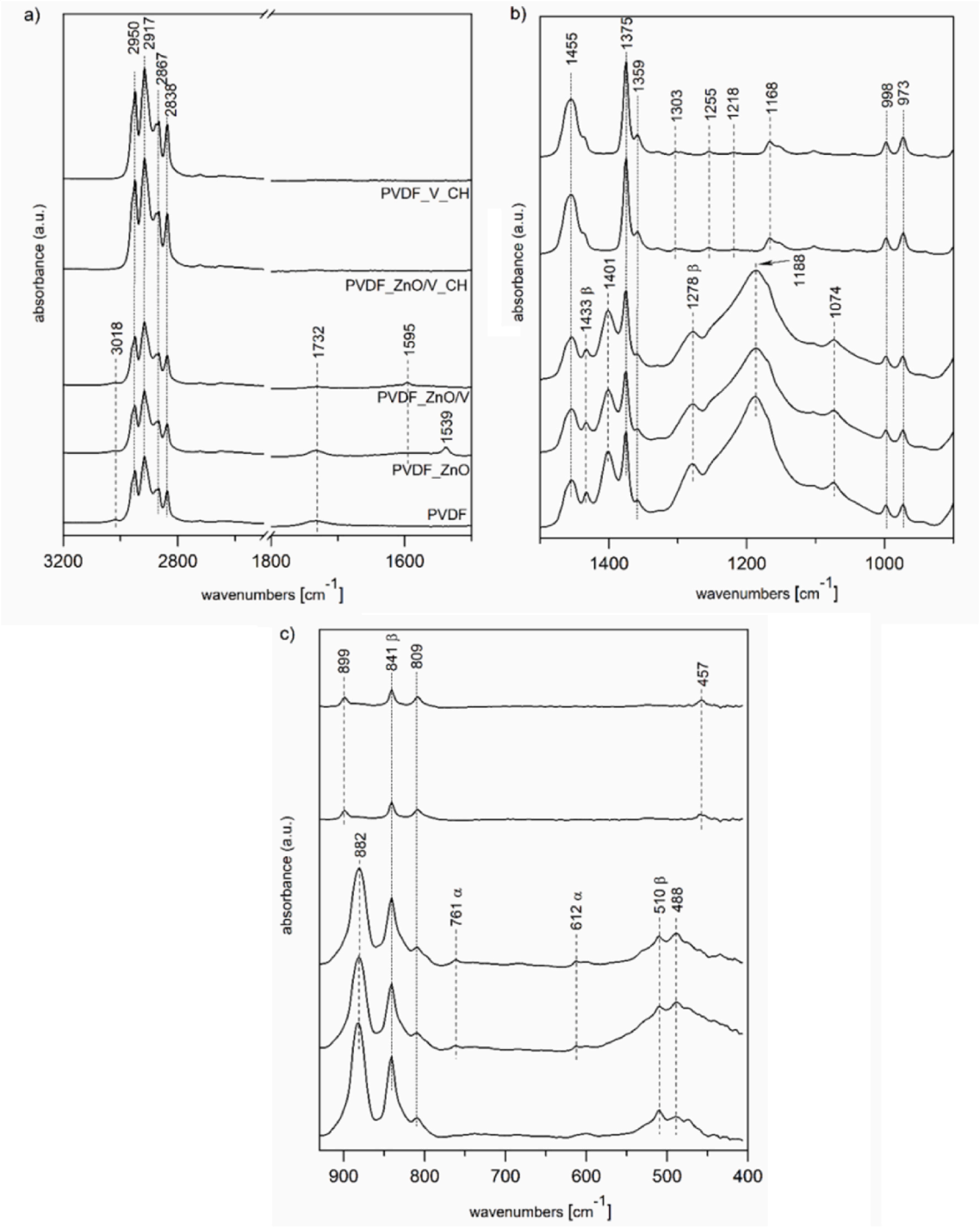

Fig. 5. FTIR spectra of the PVDF nanofiber materials in regions a) 3200-1500 cm^{-1}, b) 1500-900 cm^{-1}, c) 900-400 cm^{-1}.

curved or adjacent to nanofibers of larger diameters. The ZnO nanoparticles agglomerates formed separated spherical and clearly demarcated particles, which were coated with a PVDF layer. The nanofibers adjacent to the center of the ZnO nanoparticles agglomerates were curved, which had the tendency to unite and form fibrous smooth bands. The presence of the ZnO nanoparticles inside the PVDF drops was confirmed by EDS elemental analysis, which measured 2.7 wt% Zn, 7.3 wt% O, 60.9 wt% C and 29.1 wt% F. Despite this, the nanofiber diameters were in the range of 31 nm (Dmin) - 154 nm (Dmax).

The ZnO/V a ZnO/V_CH nanofillers fractions smaller than 500 nm were embedded into the PVDF fibers and did not present obvious changes on the fiber surface. The bigger fractions were distributed uniformly along the surface of the polymeric fiber without formation of aggregates. The fibers were smooth, straight and continuous. In the case of the PVDF_V_CH nanofiber material, a double structural interaction between the V_CH nanofiller and the PVDF polymer can be observed. PVDF formed a continuous smooth layer on the surface of V_CH nanoparticles and at the same time leads to the growth of nanofibers on the edges of these nanoparticles. The nanofibers observed mostly at these edges had variable diameters and often were curved and intertwined.

It is generally known that semi-crystalline polymer PVDF exists in three basic distinct polymorphs and FTIR technique is a very useful tool which provides valuable information about the structure and allows distinguishing between these crystalline polymorphs [25,26]. The most observed crystal structures are the thermodynamically stable α-phase and the metastable piezoelectric β-phase, which has been reported as predominantly obtained structure by solution electrospinning [27]. The FTIR spectrum of the original PVDF nanofibers (Fig. 5) shows typical bands for β-phase at 1433, 1278, 840 and 510 cm^{-1} attributed to CH_2 bending, C–F out-of-plane deformation, CH_2 rocking and CF_2 bending vibrations, respectively. In the case of PVDF_ZnO and PVDF_ZnO/V nanofibers we can observe small traces of α-phase confirmed especially by the bands at 612 and 761 cm^{-1} belonging to CF_2 bending and skeletal vibrations, moreover the previously mentioned characteristic bands for β-phase possess smaller intensity due to this phase change (Fig. 5). The bands at 1595 and 1539 cm^{-1} in PVDF_ZnO nanofiber spectrum corresponded to the asymmetric and symmetric stretching vibration of C═O originated from zinc acetate [28]. Entirely different situation becomes in the case of nanofibers samples containing CH (PVDF_ZnO/V/CH and PVDF_V/CH). We can observe (from Fig. 5), that compared to the spectrum of the original PVDF nanofibers, some bands disappeared or were shifted and some of them are new created. New peaks at 1303, 1255 and 1218 cm^{-1} prove the presence of CH and belonging to NH bending and C–N stretching vibrations [29]. The disappeared ones are 1433, 1401, 1278, 1074, 510 cm^{-1} corresponded to CH_2 bending, bending CH_2 connected with CF_2, C–F out-of-plane deformation, C–F bending and CF_2 bending vibrations, respectively [25,26,30]. Finally, the peak at 1188 cm^{-1} corresponding to CF_2–CH_2 stretching vibration in the original PVDF nanofibers spectrum was shifted to 1166 cm^{-1} together with CF_2–CH_2 bending vibration shifted from 882 to 899 cm^{-1} [31], suggesting the specific interaction of PVDF chains, specifically the negatively polarized CF_2 groups with chlorhexidine CH based on weak coulombic forces or hydrogen bonding.

3.3. Antimicrobial activity of the PVDF nanofibers materials

Antimicrobial activity of the PVDF nanofibers materials was studied by a modified AATCC 100 test method for surface-treated materials. The original PVDF nanofiber sample was used as control sample. Average numbers of colony forming units (CFU) at various time intervals are shown in Table 2.

As we mentioned above in the introduction part, PVDF is widely used polymer in the field of medicine or in the membrane separation as filters, where various contaminants can occur to form biofilm. From this reason an extensive effort was focused on development suitable antimicrobial polymeric films. Among inorganic metal oxides, the main advantages of using ZnO nanoparticles are its excellent stability and broad-spectrum antimicrobial effect. The use of vermiculite as a carrier of antimicrobials is based on its unique property, high negative layer charge leading to better adhesion of antimicrobial agents.

Although, all used nanofillers themselves showed very good antibacterial activity in the past [17], in the case of PVDF nanofiber samples made from them, only PVDF_ZnO/V_CH possessed bactericide efficacy against both investigated bacterial strains. This sample showed slightly better results against the more resistant strain *S. aureus*, after 24 h with onset already after 4 h, meanwhile in the case of *E. coli*, the onset and antibacterial efficacy were slower. Regarding the sample PVDF_V_CH, the situation looked promising against *S. aureus* after 24 h, however after a longer time interval we can again observe bacterial grow. This behavior is probably caused by better intercalation ability of CH into V interlayer space compared to intercalation of CH into ZnO/V (proved by X-ray diffraction) which is associated with better contact of antimicrobials agents (CH and ZnO) on the surface of the nanofiller ZnO/V_CH with bacteria. Moreover, there is also synergic effect of both antimicrobials in the case of PVDF_ZnO/V_CH, making this material the best in antimicrobial activity of those tested.

3.4. Mechanical properties of the PVDF nanofibers materials

The results of the tests carried out are presented in Table 3 and the tensile test curves are shown in Fig. 6. Based on the obtained results, slight differences were found in the values of parameters characterizing the PVDF nanofiber materials mechanical properties depending on the nanofiber types. The following parameters with standard deviations (S. D.) were determined: Young's modulus (E), tensile strength (R_m), maximum force (F_{max}) and maximum strain (S_{max}).

Thickness tests (thickness) of the PVDF nanofiber materials were

Table 3
Test results with standard deviations of the PVDF nanofibers materials.

Samples	E (MPa)	R_m (MPa)	F_{max} (N)	S_{max} ($mm.mm^{-1}$)	t (μm)
PVDF	409 ± 68	55 ± 17	18 ± 3	4.7 ± 0.6	11.6 ± 2.6
PVDF_ZnO	391 ± 67	48 ± 5	15 ± 2	5.7 ± 0.6	10.0 ± 2.7
PVDF_ZnO/V	375 ± 55	44 ± 20	14 ± 6	4.3 ± 1.7	9.6 ± 3.6
PVDF_ZnO/V_CH	310 ± 46	54 ± 6	17 ± 2	5.8 ± 0.7	11.1 ± 1.0
PVDF_V_CH	374 ± 71	55 ± 11	17 ± 5	5.1 ± 0.9	11.1 ± 1.6

Table 2
Efficiency of individual antibacterial agents against *S. aureus* and *E. coli*.

Samples	*S. aureus*				*E. coli*			
	Exposition time (h)							
	1	4	24	48	1	4	24	48
PVDF	231	262	>330	>330	>330	143	>330	>330
PVDF_ZnO	243	289	>330	>330	>330	247	>330	>330
PVDF_ZnO/V	234	166	>330	>330	>330	260	>330	>330
PVDF_ZnO/V_CH	290	5	0	0	174	142	19	0
PVDF_V_CH	299	220	0	>330	265	224	>330	>330

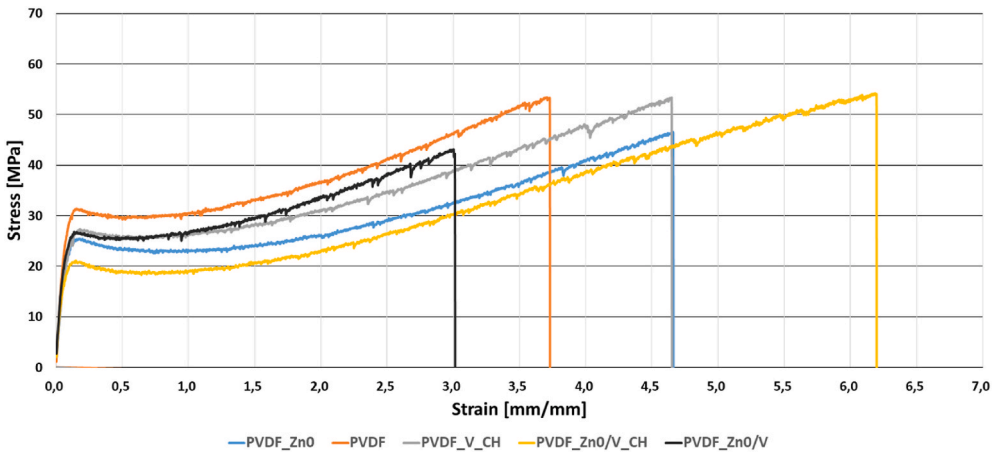

Fig. 6. The representative tensile test curves of all measured PVDF nanofiber materials.

performed before the tensile test at 5 different places of each rectangular standard samples. The measured thickness values (t) with standard deviations (S.D.) (Table 3) were evaluated in the interval value from 9.6 μm for PVDF_ZnO/V sample to the 11.6 μm for PVDF sample.

The smaller thickness values in PVDF_ZnO (t = 10.0 μm) and PVDF_ZnO/V (t = 9.6 μm) samples can be attributed to the interaction between PVDF matrix and ZnO, respectively ZnO/V nanofillers. The ZnO and ZnO/V nanofillers had have the smallest particle and agglomerates size (~10 μm, d_m) and primarily negative ζ - potential values (−39.8 mV and −20.6 mV) before electrospinning. It can be expected that ZnO and ZnO/V nanofillers react more intensively with the PVDF matrix. From the SEM micrographs is evident, that the nanofillers are mostly placed in PVDF nanofibers with the smallest thickness, which in the case of PVDF_ZnO was 30.9 nm (Dmin) and for PVDF_ZnO/V 32.9 nm. The SEM micrographs also showed that the PVDF nanofibers were situated on the surfaces of the ZnO nanoparticles agglomerates and at the edges of ZnO/V nanofillers, which can contribute to better nanofillers incorporation into the bulk of PVDF nanofiber materials and in the PVDF_ZnO and PVDF_ZnO/V nanofiber materials occurred only sporadically the beads unlike from the other PVDF nanofibrous materials.

The tensile strengths for each PVDF nanofiber materials were similar and amounted to R_m = 54 MPa. Only for the PVDF_ZnO and PVDF_ZnO/V samples, a reduction in tensile strength to the value of R_m = 48 MPa and R_m = 44 MPa was observed. The lower tensile strength value most likely resulted in a smaller sample thickness (Table 3).

The differences were observed in the case of Young's modulus (E), where it was found that the PVDF nanofiber material was characterized by the highest stiffness, corresponding to E = 409 MPa. The nanofillers decreased the stiffness to the E values ~375 MPa (for PVDF_ZnO/V and PVDF_V_CH samples) and 391 MPa for PVDF_ZnO nanofiber material. The lowest Young's modul E = 310 MPa was measured for PVDF_ZnO/V_CH nanofiber material. The results correspond also to the maximum strain values (S_{max}), where it was found that the PVDF_ZnO/V_CH nanofiber material is more susceptible to deformation (S_{max} = 5.8 mm. mm^{-1}).

It is evident that the placement of nanofillers into the bulk or on the surface of PVDF nanofiber materials have a significant effect in the evaluation of the results of mechanical properties (Young's modulus values especially). Mariya Spasova et al. [32] showed that when ZnO nanoparticles decorated the PVDF nanofiber surfaces their mechanical properties do not alter significantly. Conversely, the ZnO nanoparticles incorporated in the PVDF nanofibers significantly decreased the mechanical properties. The reason is the fact that ZnO particles act as stress concentration centres, where cracks initiate on. In our case, both the incorporation of ZnO nanoparticles into PVDF nanofibers and the minimal presence of pores in the PVDF_ZnO nanofiber material itself can contribute to this fact. The presence of ZnO agglomerates can be compared in terms of their average size to the size of nanofillers containing vermiculite nanoparticles, which can form the drop in the tensile strength and lead to the relatively reduction of Young's modulus.

The similar results of the mechanical properties tests were obtained by Ryu Nakashima [33], whose PVDF nanofibers obtained by the electrospinning method were characterized by a similar value of tensile strength in the range of R_m = 22 – 55 MPa. Javier Vicente [34], who prepared the PVDF nanofibers with nanocarbon fillers based on the tests of mechanical properties, he also found different values of tensile strength depending on the type of filler. Regardless of the type of filler used, the strength values were lower than those obtained from the pure PVDF nanofibers.

The stress-strain curves of PVDF nanofiber materials with different nanofiller types are shown in Fig. 6. The curves show the typical characteristics of thermoplastic PVDF polymers, characterised by elastic and inelastic regions separated by the yielding stress and strain [35]. As seen, the Young's modulus (E) and tensile strength (R_m) of the PVDF nanofiber materials decreased with increased diameters (D_m) of the nanofiber samples. The significant change in elongation at break was observed, which corresponded with the Smax values (Table 3). The changes in the mechanical properties of the nanofiber materials could be attributed to the combined effects of the increasing void's size and the presence of ZnO nanoparticles and V particles in PVDF nanofiber materials, which affect the internal friction in the PVDF nanofiber. Different nanofiber diameters also affect the interface interactions between the nanofibers, which improves the load transfer efficiency, resulting in a decrease in tensile strength and Young's modulus of nanofibers.

Overall, the toughness is defined as the area under the stress/strain curve and from this study correspond with the trend in increasing toughness is consistent with the amount of β phase in PVDF nanofiber materials.

4. Conclusion

The effect of four nanofillers (ZnO, ZnO/V, ZnO/V_CH and V_CH) in PVDF nanofiber materials prepared by the electropun via one-step electrospinning process was examined.

The SEM micrographs showed that the ZnO/V_CH and V/CH nanofillers with positive ζ - potential values (+23.5 mV and +19.8 mV) were incorporated into PVDF nanofibers with an average diameter (Dmean) of 108 nm for PVDF_ZnO/V_CH and 100 nm for PVDF_V_CH nanofiber materials. In contrast, ZnO and ZnO/V nanofillers with negative ζ - potential values (−39.8 mV and −20.6 mV) reacted intensively with PVDF polymer. The average nanofiber diameters (Dmean) 93 nm for PVDF_ZnO nanofiber materials and 107 nm for PVDF_ZnO/V nanofiber materials were evaluated whereas PVDF nanofibers were situated on the

surfaces of the ZnO nanoparticles agglomerates and at the edges of ZnO/V nanofillers. In PVDF_ZnO and PVDF_ZnO/V nanofiber materials occurred sporadically the beads with a round-like shape with average size around 10 μm unlike from the other PVDF nanofibrous materials. The results of the water contact angle (WCA) measurements confirmed that the presence of vermiculite in PVDF nanofiller types (ZnO/V, ZnO/V_CH and V_CH) increases the absorption of water, hence increasing its wettability. The WCA measurements confirmed that all the electrospinnning nanofiber materials exhibit surfaces with higher hydrophobicity (100° water contact angle).

FTIR analysis confirmed presence of β-phase for the original PVDF nanofibers, which is created during electrospinning process. After adding the nanofillers ZnO and ZnO/V, the small traces of α-phase were observed. Entirely different situation becomes with nanofillers containing molecule CH where the specific interaction of PVDF chains with CH based on weak coulombic forces or hydrogen bonding appeared and there was a rapid decrease in the β-phase fraction.

The PVDF nanofiber materials displayed the variable antimicrobial activity against *S. aureus* and *E. coli*. Antimicrobial activity was evaluated for all PVDF nanofiber materials against *E. coli* for a very short time of 4 h while the ZnO/V_CH nanofiller against *S. aureus* and *E. coli* showed persistent antimicrobial activity after 48 h of testing.

All nanofillers caused only a slight decrease of the Young's modulus (E) and tensile strength (R_m) values from E = 409 MPa and R_m = 55 MPa of the natural PVDF to the E = 310 MPa for PVDF_ZnO/V_CH and R_m = 44 MPa for PVDF_ZnO/V nanofiber materials. The mechanical properties contributed to the formation of the voids and PVDF droplets in PVDF layered materials.

The PVDF nanofibers materials with the ZnO - vermiculite - chlorhexidine based nanofillers represent a group of new materials with antibacterial and variable mechanical properties. Due to their easy preparation and basis weights (gsm) ranging from the 2.00 $g.m^{-2}$ for PVDF_ZnO/V_CH to the 3.35 $g.m^{-2}$ for PVDF_V_CH are suitable materials for medical materials such as filters, medical textiles - surgical drape, mouthpiece or medical mask, dressings or dental fibers and sewing materials.

Author contributions

K.Č.B., designed the work, performed the synthesis, structural changes – structural and mechanical properties, water contact angle and antimicrobial activities evaluated, writing original draft, revised and finalized the manuscript; S.H., performed the synthesis, FTIR analysis, antimicrobial activities evaluated, writing and revised the manuscript; M.H., realised and evaluated the XRDS analysis; K.H., water contact angle measured; L.P., performed the synthesis; D.K., selected the conditions for electrospinning process; J.K., investigation of mechanical properties; B.G.K. and M.B., methodology of mechanical properties.

Funding

This research received no external funding.

Declaration of competing interest

The authors declare that they have no known competing financial interests or personal relationships that could have appeared to influence the work reported in this paper.

Acknowledgments

This work was supported by the project No. SP2020/08 "Hybrid clay nanofillers for antimicrobial polymer films" and project No. SP2021/106 "Study and development of composite nanomaterials and nanofillers". Authors thank to G. Kratošová and M. Heliová for SEM micrographs, Dr. Irena Willerthová for antimicrobial activities/tests performing.

References

[1] M.L. Nallappan, M.M. Nasef, Optimization of electrospinning of PVDF scaffolds fabrication using response surface method, J. Teknol. 75 (6) (2015) 103–107.
[2] G. Kalimuldina, N. Turdakyn, I. Abay, A. Medeubayev, A. Nurpeissova, D. Adair, Z. Bakenov, Review of piezoelectric PVDF film by electrospinning and its applications, Sensors 20 (2020), 5214.
[3] B. Zaarour, L. Zhu, X. Jin, A review on the secondary surface morphology of electrospun nanofibers: formation mechanisms, characterizations, and applications, Chemistry 5 (4) (2020) 1335–1348.
[4] J.E. Dohany, Fluorine-containing polymers, poly(vinylidene fluoride), in: Kirk-Othmer Encyclopedia of Chemical Technology, John Wiley & Sons Inc., 2000.
[5] F. Liu, N.A. Hashim, Y. Liu, M.R.A. Moghareh, K. Li, Progress in the production and modification of PVDF membranes, J. Membr. 375 (2011) 1–27.
[6] Y. Li, Ch Liao, S. Ch Tjong, Electrospun polyvinylidene fluoride-based fibrous scaffolds with piezoelectric characteristics for bone and neural tissue engineering, Nanomaterials 9 (2019) 952.
[7] A. Haider, S. Haider, I.K. Kang, A comprehensive review summarizing the effect of electrospinning parameters and potential applications of nanofibers in biomedical and biotechnology, Arab. J. Chem. 11 (8) (2015) 1165–1188.
[8] D. Kimmer, P. Slobodian, D. Petras, M. Zatloukal, R. Olejník, P. Saha, Polyurethane/multiwalled carbon nanotube nanowebs prepared by an electrospinning process, J. Appl. Polym. Sci. 111 (2009) 2711–2714.
[9] S.A. Haddadi, S. Ghaderi, M. Amini, A.S.A. Ramazani, Mechanical and piezoelectric characterizations of electrospun PVDF-nanosilica fibrous scaffolds for biomedical applications, Mater. Today 5 (2018) 15710–15716.
[10] L. Yan, Y.S. Li, C.B. Xiang, S. Xianda, Effect of nano-sized Al_2O_3 particle addition on PVDF ultra filtration membrane performance, J. Membr. 276 (1–2) (2006) 162–167.
[11] S. Mansouria, T.F. Sheikholeslamia, A. Behzadmehr, Investigation on the electrospun PVDF/NP-ZnO nanofibers for application in environmental energy harvesting, J. Mater. Res. Technol. 8 (2) (2019) 1608–1615.
[12] P.P. Dorneanu, C. Cojocaru, P. Samoila, N. Olaru, A. Airinei, A. Rotaru, Novel fibrous composites based on electrospun PSF and PVDF ultrathin fibers reinforced with inorganic nanoparticles: evaluation as oil spill sorbents, Polym. Adv. Technol. 29 (2018) 1435–1446.
[13] J.A. Princea, G. Singha, D. Ranab, T. Matsuurab, V. Anbharasia, T. S. Shanmugasundaram, Preparation and characterization of highly hydrophobic poly(vinylidene fluoride)-Clay nanocomposite nanofiber membranes (PVDF-clay NNMs) for desalination using direct contact membrane distillation, J. Membr. 397 (2012) 80–86.
[14] Y. Zhai, X. Wang, Y. Chen, X. Sang, H. Liu, J. Sheng, Y. Wu, X. Wang, L. Li, Multiscale-structured polyvinylidene fluoride/polyacrylonitrile/vermiculite nanosheets fibrous membrane with uniform Li^+ flux distribution for lithium metal battery, J. Membr. 621 (2021), 118996.
[15] K. Kim, S.H. Ji, B.S. Park, J.S. Yun, High surface area flexible zeolite fibers based on a core-shell structure by a polymer surface wet etching proces, Mater. Des. 158 (2018) 98–105.
[16] K. Buruga, H. Song, S. Jin, N. Bolan, T.K. Jagannathan, K.H. Kim, A review on functional polymer-clay based nanocomposite membranes for treatment of water, J. Hazard Mater. 379 (2019), 120584.
[17] K. Čech Barabaszová, S. Holešová, K. Šulcová, M. Hundáková, B. Thomasová, Effects of ultrasound on zinc oxide/vermiculite/chlorhexidine nanocomposite preparation and their antibacterial activity, Nanomaterials 9 (9) (2019), 1309.
[18] H.A. Sani, M.B. Ahmad, M.Z. Hussein, N.A. Ibrahim, A. Musa, T.A. Saleh, Preparation of ZnO-supported 13X zeolite particles and their antimicrobial mechanism, Process Saf. Environ. Protect. 32 (22) (2017) 4232–4240.
[19] N. Khaorapapong, N. Khumchoo, M. Ogawa, Preparation of zinc oxide-montmorillonite hybrids, Mater. Lett. 65 (2011) 657–660.
[20] E. Hosono, S. Fujihara, T. Kimura, H. Imai, Non-basic solution routes to prepare ZnO nanoparticles, J. Sol. Gel Sci. Technol. 29 (2004) 71–79.
[21] D. Luković Golić, G. Branković, M. Počuča Nešić, K. Vojisavljević, A. Rečnik, N. Daneu, S. Bernik, M. Šćepanović, D. Poleti, Z. Branković, Structural characterization of self-assembled ZnO nanoparticles obtained by the sol-gel method from $Zn(CH_3COO)_2{\cdot}2H_2O$, Nanotechnology 22 (2011), 395603.
[22] K. Čech Barabaszová, S. Holešová, M. Hundáková, A. Kalendová, Tribo-mechanical properties of the antimicrobial low-density polyethylene (LDPE) nanocomposite with hybrid ZnO-Vermiculite-Chlorhexidine nanofillers, Polymers 12 (2020), 2811.
[23] K. Čech Barabaszová, M. Valášková, Characterization of vermiculite particles after different milling techniques, Powder Technol. 239 (2013) 277–283.
[24] N.T. Skipper, A.K. Soper, J.D.C. McConnell, The structure of interlayer water in vermiculite, J. Chem. Phys. 94 (1991), 5751.
[25] X. Cai, T. Lei, D. Sun, L. Lin, A critical analysis of the α, β and γ phases in poly (vinylidene fluoride) using FTIR, RSC Adv. 7 (25) (2017) 15382–15389.
[26] Y. Bormashenko, R. Pogreb, O. Stanevsky, E. Bormashenko, Vibrational spectrum of PVDF and its interpretation, Polym. Test. 23 (7) (2004) 791–796.
[27] ChM. Azzaz, L.H.C. Mattoso, N.R. Demarquette, R.J. Zednik, Polyvinylidene fluoride nanofibers obtained by electrospinning and blowspinning: electrospinning enhances the piezoelectric β-phase – myth or reality? J. Appl. Polym. Sci. 138 (10) (2021), e49959.
[28] H. Yin, P.S. Casey, ZnO nanorod composite with quenched photoactivity for UV protection application, Mater. Lett. 121 (2014) 8–11.

[29] M. Samlíková, S. Holešová, M. Hundáková, E. Pazdziora, Ľ. Jankovč, M. Valášková, Preparation of antibacterial chlorhexidine/vermiculite and release study, Int. J. Miner. Process. 159 (2017) 1–6.
[30] T. Boccaccio, A. Bottino, G. Capannelli, P. Piaggio, Characterization of PVDF membranes by vibrational spectroscopy, J Membr. 210 (2) (2002) 315–329.
[31] E. Thomas, C. Parvathy, N. Balachandran, S. Bhuvaneswari, K.P. Vijayalakshmi, B. K. George, PVDF-ionic liquid modified clay nanocomposites: phase changes and shish-kebab structure, Polymers 115 (2017) 70–76.
[32] M. Spasova, N. Manolova, N. Markova, I. Rashkov, Tuning the properties of PVDF or PVDF-HFP fibrous materials decorated with ZnO nanoparticles by applying electrospinning alone or in conjunction with electrospraying, Fibers Polym. 18 (4) (2017) 649–657.
[33] R. Nakashima, K. Watanabe, Y. Lee, B.S. Kim, I.S. Kim, Mechanical properties of poly(vinylidene fluoride) nanofiber filaments prepared by electrospinning and twisting, Adv. Polym. 32 (S1) (2013) E44–E52.
[34] V. Javier, P. Costa, S. Lanceros-Mendez, J.M. Abete, A. Iturrospe, Electromechanical properties of PVDF-based polymers reinforced with nanocarbonaceous fillers for pressure sensing applications, Materials 12 (21) (2019) 3545.
[35] C.M. Costa, V. Sencadas, I. Pelicano, F. Martins, J.G. Rocha, S. Lanceros-Mendez, Microscopic origin of the high-strain mechanical response of poled and non-poled poly(vinylidene fluoride) in the β-phase, J. Non-Cryst. Solids 354 (2008) 3871–3876.